Ultracentrifuge and Circular Dichroism Studies of Folding Equilibria in a Retro GCN4-like Leucine Zipper

Marilyn Emerson Holtzer,* Emory Braswell,† Ruth Hogue Angeletti,‡ Lisa Mints,‡ Dan Zhu,† and Alfred Holtzer*
*Department of Chemistry, Washington University, St. Louis, Missouri 63130-4899; †Department of Molecular and Cell Biology, University of Connecticut, Storrs, Connecticut 06269-3125; and ‡Laboratory for Macromolecular Analysis, Albert Einstein College of Medicine, Bronx, New York 10461 USA

ABSTRACT Equilibrium ultracentrifuge and circular dichroism (CD) studies of a retropeptide of a GCN4-like leucine zipper in neutral saline buffer are reported as functions of temperature. Ultracentrifuge results indicate the presence of three oligomeric species: monomer, dimer, and tetramer, in quantifiable amounts, and the data provide values for the standard ΔG, ΔH, and ΔS for interconversion. CD at 222 nm displays the strong concentration dependence characteristic of dissociative unfolding, but also shows a helicity far below that of the parent propeptide. Remarkably enough, the CD at 222 nm shows an extremum in the region between 0 and 20°C. At higher T, the usual cooperative unfolding is observed. Comparable data are presented for a mutant retropeptide, in which a single asparagine residue is restored to the characteristic heptad position it occupies in the propeptide. The mutant shows marked differences from its unmutated relative in both thermodynamic properties and CD, although the oligomeric ensemble also comprises monomers, dimers, and tetramers. The mutant is closer in helicity to the parent propeptide but is less stable. These findings do not support either of the extant views on retropeptides. The behavior seen is consistent neither with the view that retropeptides should have the same structure as propeptides nor with the view that they should have the same structure but opposite chirality. The simultaneous availability of oligomeric population data and CD allows the latter to be dissected into individual contributions from monomers, dimers, and tetramers. This dissection yields explanations for the observed extrema in curves of CD (222 nm) versus T and reveals that the dimer population in both retropeptides undergoes "cold denaturation."

INTRODUCTION

Retropeptides, in which the sequence of a known protein or peptide is expressed backward, have attracted a lot of attention for their possible clinical significance (Chorev and Goodman, 1995). Physical studies of folding equilibria in such peptides, however, are relatively scarce. This is remarkable, because they would seem to present attractive objects for testing our ideas on the physical basis of conformation. Retropeptides clearly differ physically from their propeptide parents, yet the two have many features in common, including composition, chirality, and spacing of their constituent amino acids. They therefore allow comparison of peptide conformation in a context wherein many important variables are strictly controlled. The lack of information on the structural preferences of retropeptides is all the more noteworthy, considering the vast number of studies of propeptide mutants of biological peptides.

Theorists have opined variously on the effect of retroexpression on conformational preferences. Views range from the prediction that their preferred conformation should be very much like that of the propeptide parent (Olszewski et al., 1996) to the notion that a retropeptide should have the same structure as the propeptide, but with reversed chirality (Guptasarma, 1992). Although some evidence is extant (Ido et al., 1997; McDonnell et al. 1997), the validity of these ideas does not seem to have been thoroughly tested experimentally by detailed physical studies.

Coiled coils, in which right-handed α-helical chains are arranged in parallel and given a left-handed supertwist, constitute a class of peptides well suited to such a test, because the features of the sequence that lead to that preferred conformation are better understood than any other peptide structural type (Crick, 1953; McLachlan and Stewart, 1995; Lupas, 1996). The coiled-coil conformation is dictated by a pseudo-repeating heptad of amino acids, designated *abcdefg*, in which the *a* and *d* residues are hydrophobic and the *e* and *g* residues are oppositely charged. This spacing of the hydrophobes lends an amphipathicity to the helix that favors side-to-side association. Supplementary interhelical charge-charge interactions supposedly ensure parallel association.

One further feature of coiled coils renders their use in assessing the effects of retroexpression even more attractive. Because an *a* residue is, by definition, the one after which two residues intervene before the next canonical hydrophobe is reached, whereas a *d* residue is one after which three intervene, reversal of the sequence corresponds to the transformations $a \leftrightarrow d$, $b \leftrightarrow c$, $e \leftrightarrow g$, $f \leftrightarrow f$; i.e., *a* residues become *d* and vice versa, etc. Only *f* residues retain their heptad designation. Thus retroexpression also conserves, to a zeroth approximation, the hydrophobic interface and the charge-charge interactions. However, in view of the different roles ascribed to *a* and *d* hydrophobes in the interface (O'Shea et al., 1991; Harbury et al., 1993), this

Received for publication 1 November 1999 and in final form 29 December 1999.

Address reprint requests to Dr. Alfred Holtzer, Department of Chemistry, Washington University Campus Box 1134, One Brookings Drive, St. Louis, MO 63130-4899. Tel.: 314-935-6572; Fax: 314-935-4481; E-mail: holtzer@wuchem.wustl.edu.

0006-3495/00/04/2037/12 $2.00

could have serious structural consequences. Nor is it certain that the structure would be indifferent to reversing the signs of the charges on the *e* and *g* residues. Only experiment can provide the answer.

Despite the appeal of coiled coils as tests of these ideas, only one prior study of retro-coiled coils is extant, to our knowledge (Liu et al., 1998). However, it employed a somewhat different peptide in a medium far from physiological; it is discussed below. Our own studies employ, throughout, the neutral saline phosphate buffer solvent $(NaCl)_{100}(NaPi)_{50}(7.4)$, wherein we designate complex aqueous solvent media by giving the formula for each solute with its millimolarity as subscript, followed by the pH in parentheses.

We report here on thermal unfolding equilibria in two retro-GCN4-like peptides whose propeptide parent has been thoroughly studied (Lovett et al., 1996; Holtzer et al., 1997; d'Avignon et al., 1998, 1999). This parent, GCN4-lzK, has a sequence that is closely related to that of the native leucine zipper, GCN4-lz, of an important transcription factor (O'Shea et al., 1989). GCN4-lz and GCN4-lzK differ in that the latter bears conservative mutations at four sites: R1K, H18K, R25K, and R33K. Both GCN4-lz and GCN4-lzK form stable, parallel, two-stranded coiled coils. The sequence of the retropeptide to GCN4-lzK, r-GCN4-lzK, is shown in Fig. 1.

Because residue N16(*a*) has been implicated in the propeptides as an important determinant in dimer formation via interhelical hydrogen bonding (Lumb and Kim, 1995), it seems advisable to examine the effects of moving that asparagine residue, which appears as N18(*d*) in the retro version. Consequently, we also synthesized the L15N/N18L mutant of r-GCN4-lzK. This permutation has the effect of placing the asparagine in an *a* heptad position, while moving a nearby leucine to a *d* position, each thus being placed in the normal heptad position they occupy in the native leucine zipper propeptides. The amino acid numbering of retropeptides can be confusing. It helps to recognize that the residue number of any amino acid in a retropeptide may be determined from the number, *i*, of that residue in the propeptide via $n + 1 - i$, wherein *n* is the total number in the peptide. In the present case, this becomes $34 - i$. The sequence of the L15N/N18L mutant retropeptide, here called mr-GCN4-lzK, is also shown in Fig. 1.

Because the oligomerization state and conformational states of these peptides are equally important, we chose to study the equilibrium ultracentrifugation and circular dichroism (CD) of these two retropeptides as functions of temperature. As will be seen, neither of the two extreme ideas described above to deduce the structure of the retropeptide from that of its propeptide parent suffices to explain the results. A reliable predictive scheme for handling the reversal of sequence remains to be developed.

MATERIALS AND METHODS

Peptide synthesis, purification, and characterization

Peptides were prepared by solid -phase synthesis on an Applied Biosystems 433A peptide synthesizer, using *N*-9-fluorenylmethyloxycarbonyl (Fmoc) strategies and Rink Amide resins (Advanced ChemTech, Louisville, KY). N-terminal acetylation was effected, before deprotection and cleavage, by reacting with acetic anhydride in diethylamine and *N*-hydroxybenzotriazole dissolved in *N*-methylpyrrolidone. Peptides were deprotected and cleaved from the resin by incubation for 2 h in trifluoroacetic acid:thioanisole:ethanedithiol:phenol:water :: 83.3:4.2:2.1:6.2:4.2. The product was precipitated and washed with *tert*-butyl methyl ether (4°C) and lyophilized before further purification. Each peptide was characterized by high-performance liquid chromatography, amino acid analysis, electrospray ionization, and matrix-assisted laser-desorption ionization mass spectrometry. After final purification via high-performance liquid chromatography, the products were 99% pure and had measured molecular masses within ±1 Da of the expected value, 3944.7 Da.

Equilibrium ultracentrifugation

All sedimentation studies were carried out using as solvent the aqueous saline phosphate buffer $(NaCl)_{100}(NaPi)_{50}(7.4)$. Solutions at different concentrations in the range 25–500 μM (as chains) were loaded into the three solution channels of 12 -mm Beckman double-sector, quartz-window, analytical ultracentrifugation cells to create solution column heights of 4–6 mm. This required 240–300 μl of solution. High-density fluorocarbon oil (no. FC-43; Minnesota Mining and Manufacturing Co.), 10–30 μl, was added to improve the visibility of the lower part of the solution. The solvent buffer (~20 μl more than the total volume in the sample compartment) was loaded into each solvent compartment.

Solutions were centrifuged in a Beckman XLA/I analytical ultracentrifuge at 3 000 rpm to determine the absorbance (at 230, 250, and 275 nm) of each solution at its loading concentration. The resulting extinction coefficients were used to normalize the data to one another for the global fit. The high extinction coefficient of the peptide, combined with the high signal-to-noise ratio of the XLA/I at 230 nm, make this wavelength a desirable choice for low concentration measurements. The steep dependence of the extinction coefficient on wavelength (in the low-wavelength region), combined with mechanical inaccuracies in the monochrometer, can lead to a dependence of the actual wavelength scanned on the radius. However, the absorption was found to be constant across the cell at low speed (before detectable sedimentation occurred), justifying the use of this wavelength.

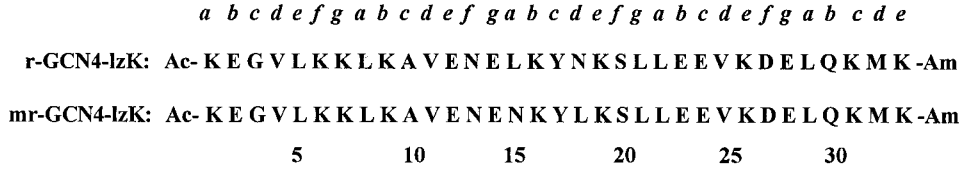

FIGURE 1 Amino acid sequences of retropeptides. *Top sequence*: r-GCN4-lzK, retropeptide of GCN4-lzK. *Bottom sequence*: mr-GCN4-lzK, the L15N/N18L mutant of r-GCN4-lzK. Heptad designation letters for these retropeptides are at the very top.

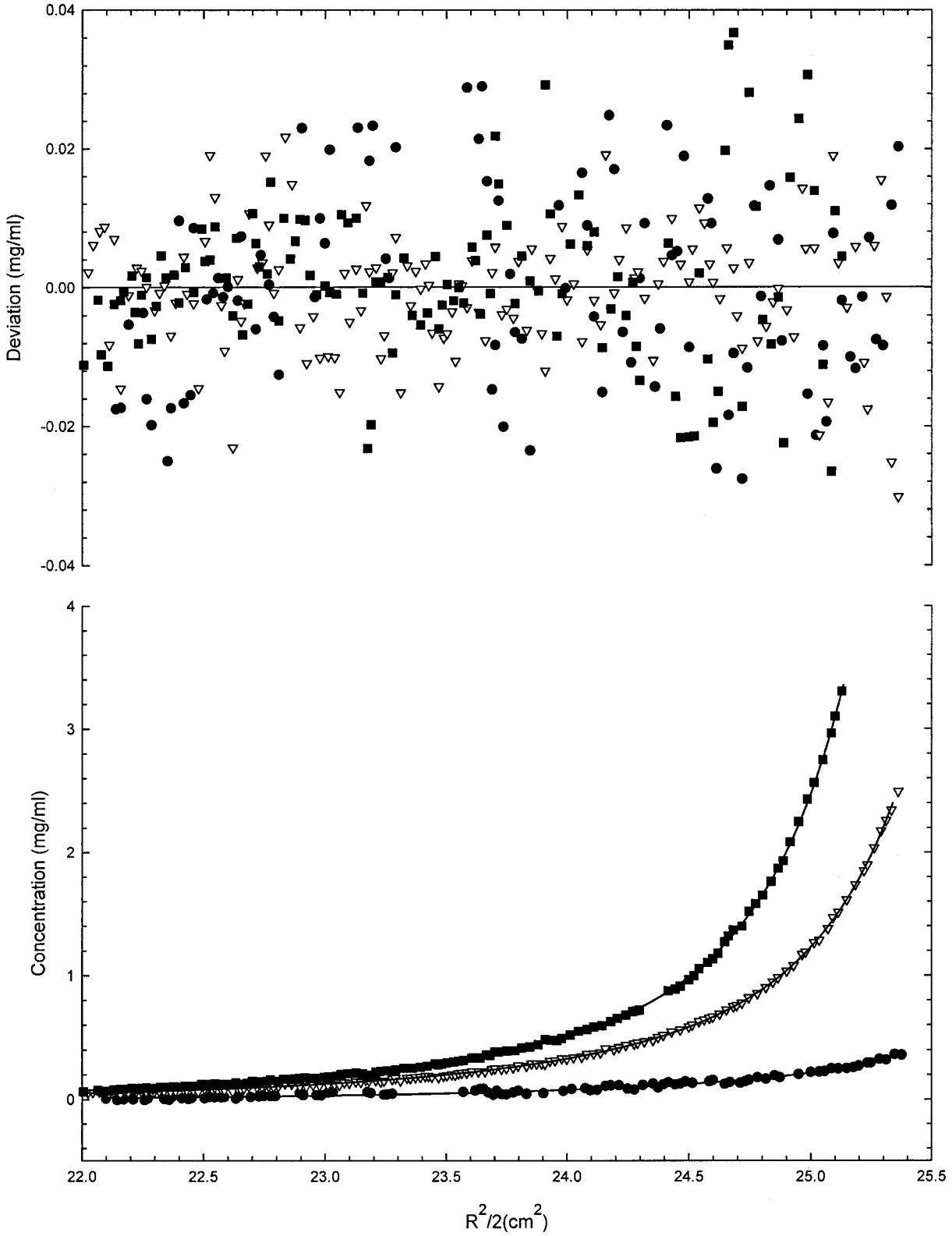

FIGURE 2 Sedimentation equilibrium data for r-GCN4-lzK in $(NaCl)_{100}(NaPi)_{50}(7.4)$ at 37°C. Rotor speed: 48,000 rpm; loading concentrations (mg/ml): 0.1 (●), 0.3 (▽), 0.5 (■). Every other point has been removed for clarity. One mg/ml corresponds in this peptide to 253 μM. Curves through the data are best fits to the monomer-dimer-tetramer model. Resulting averaged thermodynamic parameters are given in Table 1. The upper portion shows residuals from the fit. The RMS error of the fit corresponds to 8 μg/ml. Under these conditions, the tetramer predominates above 1.5 mg/ml, the monomer below 0.76. The dimer never predominates; its maximum content is 15%.

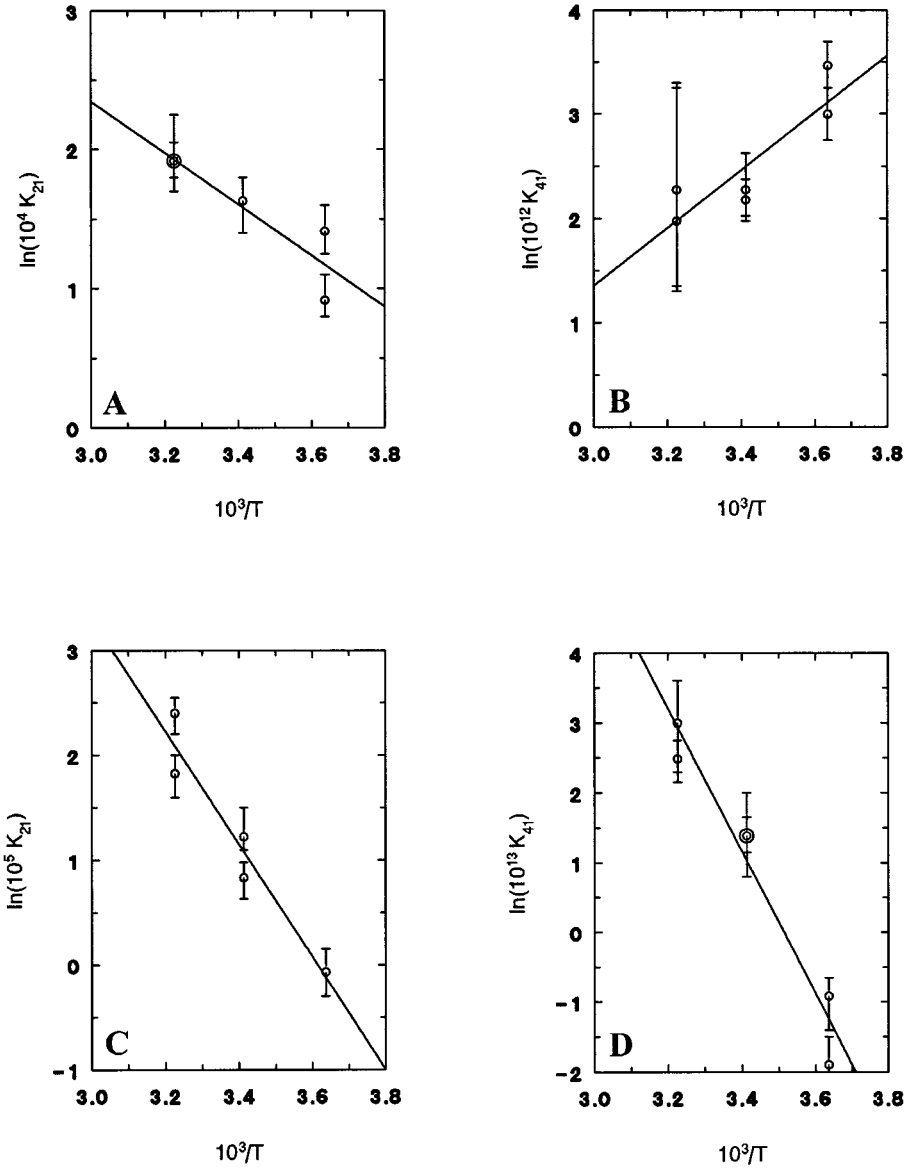

FIGURE 3 van't Hoff plots of ultracentrifuge-determined equilibrium constants for dimer (K_{21}) and tetramer (K_{41}) dissociation into monomers. (*A* and *B*) r-GCN4-lzK. (*C* and *D*) mr-GCN4-lzK. Error bars are 95% confidence limits (two standard deviations).

Solutions were then centrifuged at 48 ,000 rpm at 2°C. The concentration gradient was measured by absorbance at 275 and 230 nm for a 25 μM sample and at 250 nm for a 500 μM sample. Data were acquired at ~10 -μm intervals down the cell, with a typical error of ~ ± 0.006 (95% confidence interval) absorbance units, corresponding at 275 nm to ± 0.5 μM. Data were taken every 3–4 h to test for equilibrium, which was reached in ~ 40 h, as judged by the constancy of the gradient according to the program MATCH. After equilibrium data were taken at 2°C, the temperature was raised to 20°C and centrifugation continued at the same speed. Final data at 20°C were taken when the new equilibrium was reached (in ~ 30 h). Finally, the temperature was raised to 37°C, and data were taken upon attainment of equilibrium (~ 26 h). For some solutions at this highest temperature, we also observed some slow decrease in the concentration across the cell with time, perhaps indicating the formation of some higher aggregates that sediment out of solution. The effect was too small and variable to quantitate. Moreover, it did not affect the slopes and therefore left the fits unchanged.

The specific volume for both peptides was estimated from the amino acid composition, by the method of Cohn and Edsall (1943), to be 0.769 ml/g. The solvent density was estimated from density tables to be 1.0110, 1.0093, and 1.0043 g/ml at 2, 20, and 37°C, respectively. The three data sets from a given run at a given temperature were combined and fit globally with the nonlinear least-squares program NONLIN (Johnson et al., 1981) for the following models: ideal-dilute single species, monomer-dimer, monomer-trimer, monomer-dimer-trimer, and monomer-dimer-tetramer. The molar mass of the monomer was constrained to the expected value, 3945 Da. The MATCH and NONLIN programs were written by J. Lary and David A. Yphantis, and are available on the anonymous FTP site spin6.mcb.uconn.edu.

Occasionally, leakage in one solution channel occurred, nullifying that channel as a source of useful data. The global fit then only comprised data from the remaining two channels. The entire experimental protocol was duplicated with newly prepared samples several months later, doubling the total data set.

CD

CD was determined using a Jasco (Easton, MD) J500A spectropolarimeter with computer control via a Jasco IF-500 interface. All procedures have

been described (Holtzer et al., 1995). We used the same aqueous solvent as was used in the ultracentrifuge studies, $(NaCl)_{100}(Na\ Pi)_{50}(7.4)$.

RESULTS

Equilibrium ultracentrifugation

Experiments were performed at 2, 20, and 37°C, covering the entire feasible experimental range of the ultracentrifuge. A sample of the data for the r-GCN4-lzK peptide is shown in Fig. 2. By far the best fit of all of the data for both peptides was obtained with a monomer-dimer-tetramer equilibrium population. In Fig. 2, the global fit for the three solutions in that run at 37°C is also shown (*solid curve*); the residuals indicate that the fit is quite satisfactory.

The resulting equilibrium constants for dissociation reactions of the form: $A_2 \leftrightarrows 2A$ and $A_4 \leftrightarrows 4A$ for each peptide are displayed as van't Hoff plots in Fig. 3. Two outlying points (not shown), one for each peptide, were omitted from the fits, because each deviated from the line defined by the remaining five by over three times the deviation of any of the others. The best (least-squares) lines through the data are given by the following equations.

For r-GCN4-lzK:

$$\ln(10^4 K_{21}) = -1843(1/T) + 7.873, \quad (1)$$

and

$$\ln(10^{12} K_{41}) = 2760(1/T) - 6.927, \quad (2)$$

while for mr-GCN4-lzK:

$$\ln(10^5 K_{21}) = -5373(1/T) + 19.42, \quad (3)$$

and

$$\ln(10^{13} K_{41}) = -10{,}190(1/T) + 35.81, \quad (4)$$

wherein K_{21} and K_{41} have nominal units of mol/L and $(mol/L)^3$, respectively, and T is the Kelvin temperature. These algorithms allow calculation of best values of the equilibrium constants at any T in the range of the data and of the corresponding standard enthalpies and entropies of the dissociation reactions. The latter thermodynamic quantities will be presented and discussed below. It suffices to mention here that it is an unusual feature of these results that the enthalpy for the dissociation of the r-GCN4-lzK tetramer is negative, resulting in an increase in the tetramer relative to monomer as the temperature rises. As will also be seen below, this oddity has serious consequences for the optical properties of the system.

CD

Sample CD spectra of r-GCN4-lzK are shown in Fig. 4. The experimentally feasible temperature range for CD far exceeds that for the ultracentrifuge. The spectra at low T, interpreted conventionally, clearly show evidence (the minima at 208 and 222 nm) of the presence of considerable amount of right-handed α-helix, the usual helix chirality found in peptides made from L-amino acids. However, unlike its parent propeptide and other two-stranded coiled coils, such as tropomyosin, r-GCN4-lzK does not show anywhere near full helicity at lower temperatures, nor is there a sharp isodichroic point in the 203–205 -nm region (Fig. 4, *inset*). The latter suggests that there are more than two local peptide-group environments in the conformational population. The same is true of the mutant mr-GCN4-lzK peptide (spectra not shown), although the values at 222 nm and low T indicate greater helicity than in r-GCN4-lzK.

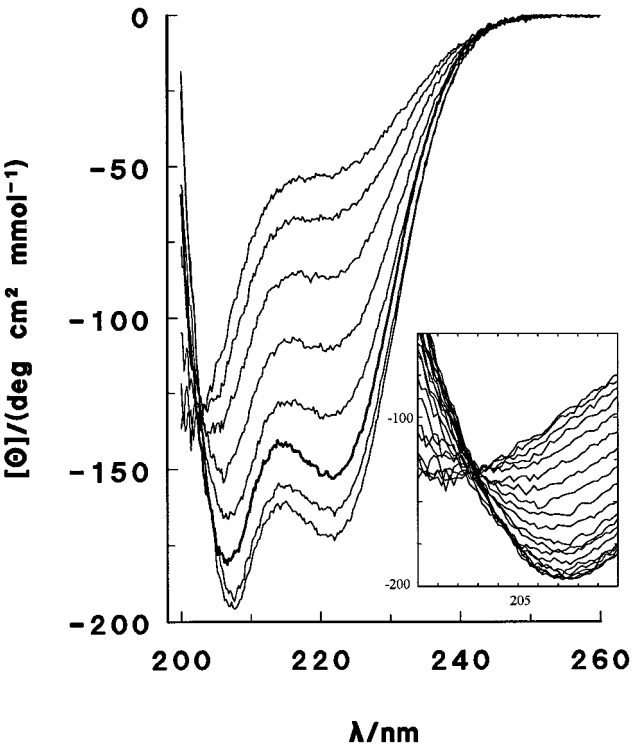

FIGURE 4 Sample CD spectra of r-GCN4-lzK at various temperatures (°C). The solvent is $(NaCl)_{100}(NaPi)_{50}(7.4)$. Temperatures are, reading upward at 222 nm, 15.1, 24.8, 2.2 (*heavy curve*), 35.4, 40.7, 46.1, 51.4, 59.4. *Inset*: Spectra near the usual isodichroic point in coiled coils (203–205 nm). Temperatures are, reading upward at 207.5 nm, 8.6–24.8 (*group of five close-lying curves*), 5.5, 2.2, 30.1, 32.8, 35.4, 38.1, 40.7, 43.4, 46.1, 48.8, 51.4, 54.1, 56.7, 59.4.

Using the negative of the values at 222 nm, in the usual way, as a measure of helix content, we show them as a function of T in Figs. 5 (r-GCN4-lzK) and 6 (mr-GCN4-lzK). As these figures (as well as Fig. 4) show, the thermal unfolding of the r-peptide is extraordinary in that it displays a maximum in helicity near room temperature that is more pronounced at moderate concentrations. The corresponding curves for the mutant retropeptide, on the other hand, not only show higher general helix content, but are more conventional, declining monotonically with T, except for a hint of a maximum at the very lowest temperatures (near 6°C)

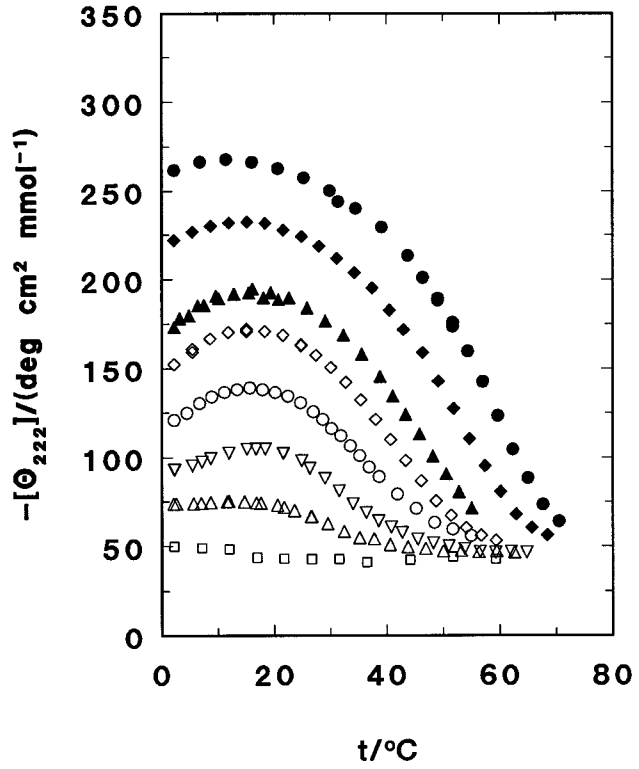

FIGURE 5 Negative of the mean residue ellipticity at 222 nm versus Celsius temperature for r-GCN4-lzK. Reading upward at 20°C, peptide concentrations (μM in total chains) are 3.0, 31.2, 59.2, 94.0, 192, 319, 596, 1032.

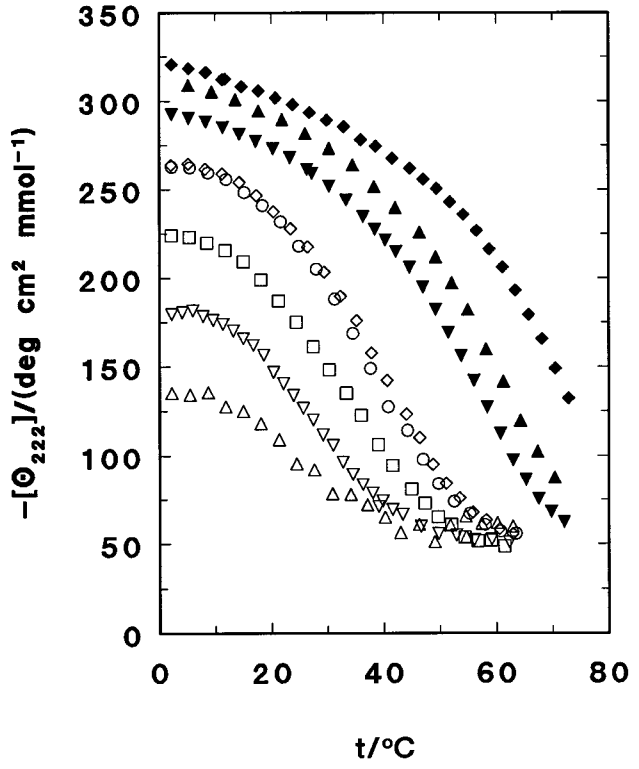

FIGURE 6 Negative of the mean residue ellipticity at 222 nm versus Celsius temperature for mr-GCN4-lzK. Reading upward at 20°C, peptide concentrations (μM in total chains) are 1.5, 3.3, 10.9, 20.9 (○), 31.5 (◇), 330, 600, 2300.

and concentrations (near 3 μM). Both retropeptides show strong concentration dependence of the CD at 222 nm, as expected for structures that dissociate as they unfold. At the lowest concentration (3 μM), r-GCN4-lzK shows very low, temperature-independent CD and spectra showing little helix content. Both retro- and mutant retropeptides show cooperative unfolding at elevated temperatures.

DISCUSSION

Thermodynamics of oligomerization

The temperature dependence of the equilibrium constants, given in Eqs. 1–4 above, provide values of the standard Gibbs energies, enthalpies, and entropies of the corresponding dimer-to-monomer and tetramer-to-monomer dissociation reactions, from which the tetramer-to-dimer values readily follow. All of these properties are given in Table 1 and are displayed as energy-level diagrams in Fig. 7, in which the values for the monomer have arbitrarily been set at zero.

Fig. 7 makes plain that the retropeptide differs drastically from its L15N/N18L mutant. In particular, the standard enthalpy and entropy of the mutant dimer and tetramer are, per chain, much lower, compared with their own monomer, than one finds for the retropeptide itself. The simplest interpretation of this finding is that the chains in these oligomeric folded forms are more tightly and rigidly held in mr-GCN4-lzK than in the r-GCN4-lzK.

A second striking difference is that, in r-GCN4-lzK, but not in its mutant, both the enthalpy and entropy of tetramer are greater, per chain, than for the monomer or dimer. Thus, in the range of the ultracentrifuge data, i.e., 0–37°C, increasing T favors association of the r-GCN4-lzK chains into tetramers, rather than dissociation. As is discussed below, this oddity has significant consequences for the observed CD of the retropeptide.

Retropeptide conformation

From one theoretical point of view, the conformation of a retropeptide is expected to be very similar to that of its

TABLE 1 Thermodynamic parameters for oligomerization

Peptide	ΔH°_{21}	ΔS°_{21}	ΔH°_{41}	ΔS°_{41}	ΔH°_{42}	ΔS°_{42}
r-GCN4-lzK	3.66	−2.66	−5.49	−68.7	−12.8	−63.4
mr-GCN4-lzK	10.7	15.7	20.3	11.7	−1.1	−19.7

The stoichiometric unit (su) is $A_2 \rightleftarrows 2A$ for the subscript 21; $A_4 \rightleftarrows 4A$ for the subscript 41; $A_4 \rightleftarrows 2A_2$ for the subscript 42. Enthalpies are in kcal/su; entropies are in cal/(K-su).

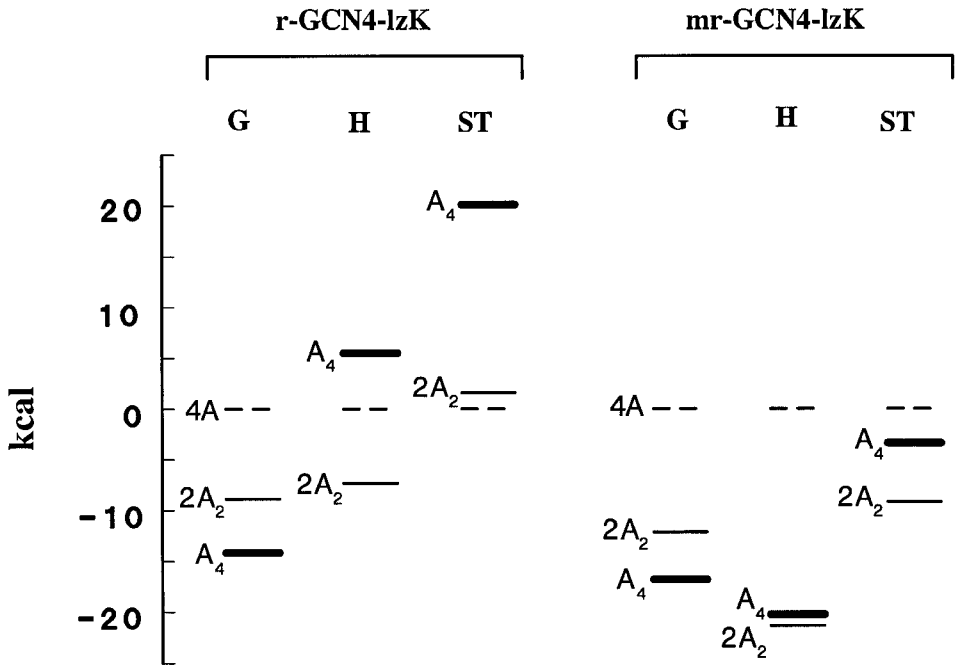

FIGURE 7 Energy levels of oligomers from thermodynamic data of Table 1. Levels are given for standard Gibbs energy, enthalpy, and entropy-temperature product (at 20°C) for both r-GCN4-lzK (*left*) and mr-GCN4-lzK (*right*) in kcal per four chains for all. Levels for monomers (– – –) have been set to zero arbitrarily.

propeptide parent (Olszewski et al., 1996). In view of the strong similarity of pro- and retropeptides in amino acid composition, side-chain interval, chain length, and net charge, this proposal is not without intuitive appeal. However, it must be noted that there are also significant differences. In a right-handed α-helix made from L-amino acids, the C^{α}-C^{β} bond vectors have a strong component along the helix axis that points toward the amino terminus. Thus, for example, in a sequence segment, say, —LIVE—, the valine side chain points in the general axial direction of the isoleucine. In the corresponding retrosequence of L-amino acids, —EVIL—, the valine points toward the glutamate instead.

In any case, it is immediately evident from our CD and ultracentrifuge data that this idea cannot be nearly correct in the present instance. The parent propeptide coiled coil, GCN4-lzK, is dimeric and has a very high helix content at lower temperatures (Lovett et al., 1996). Its retro version, r-GCN4-lzK, on the other hand, has considerable monomer-chain content, even at, say, 300 μM, and a significant tetrameric content as well. Differences are also manifested in the CD, which at 20°C and 300 μM, for example, is only two-thirds of the value observed for the propeptide parent. Moreover, the retropeptide shows a sensitivity of its structure to concentration that exceeds that of the parent, and a maximum in the helix content near room temperature that has no counterpart in the data for the propeptide. Clearly, the proposal that retro- and propeptide relatives should have similar structures fails badly here.

Undoubtedly, this idea fails in part because r-GCN4-lzK is no longer a leucine zipper. Leucines appear canonically in the *d* heptad positions in leucine zippers but shift to *a* in the retro version. Further difficulty may result from the corresponding shift of N16(*a*) of the propeptide, where its hydrogen bonding favors dimers (Lumb and Kim, 1995), to N18(*d*) in the retropeptide. However, this latter shift cannot be the sole difficulty. Although the mutant retropeptide, mr-GCN4-lzK, is somewhat more similar in CD to its parent, GCN4-lzK, it also has an appreciable tetramer presence not evident in the parent. Moreover, although at 222 nm the CD of mr-GCN4-lzK is rather similar to that for GCN4-lzK at the lowest temperatures and highest concentrations, the former is much more sensitive to concentration. Finally, there is a hint, at lower T ($\sim$ 6°C) and concentrations ($\sim$3 μM), in the mutant retropeptide of the CD extremum that is seen more prominently in the retropeptide itself. Indeed, even up to $\sim$330 μM, the curves of Fig. 6 are relatively flat at lower T. This feature is not only absent in GCN4-lzK, but, to our knowledge, has not previously been seen in leucine zippers or other coiled coils comprising like chains.

A very different theoretical point of view has given rise to a very different prediction for the conformational relationship of pro- and retro peptides, a prediction that stems from the similarity of the bond angles around >N-H and >C=O groups in a peptide chain (Guptasarma, 1992). This similarity, it is argued, implies that permutation of these groups in each peptide bond would therefore produce little or no change in a peptide's equilibrium conformation. Because such a permutation transforms a propeptide chain made from L-amino acids into the corresponding retropeptide of D-amino acids, the proposal predicts that two such peptides would have the same structure. That is, if a certain pro-L-peptide sequence forms a right-handed α-helix, the theorem

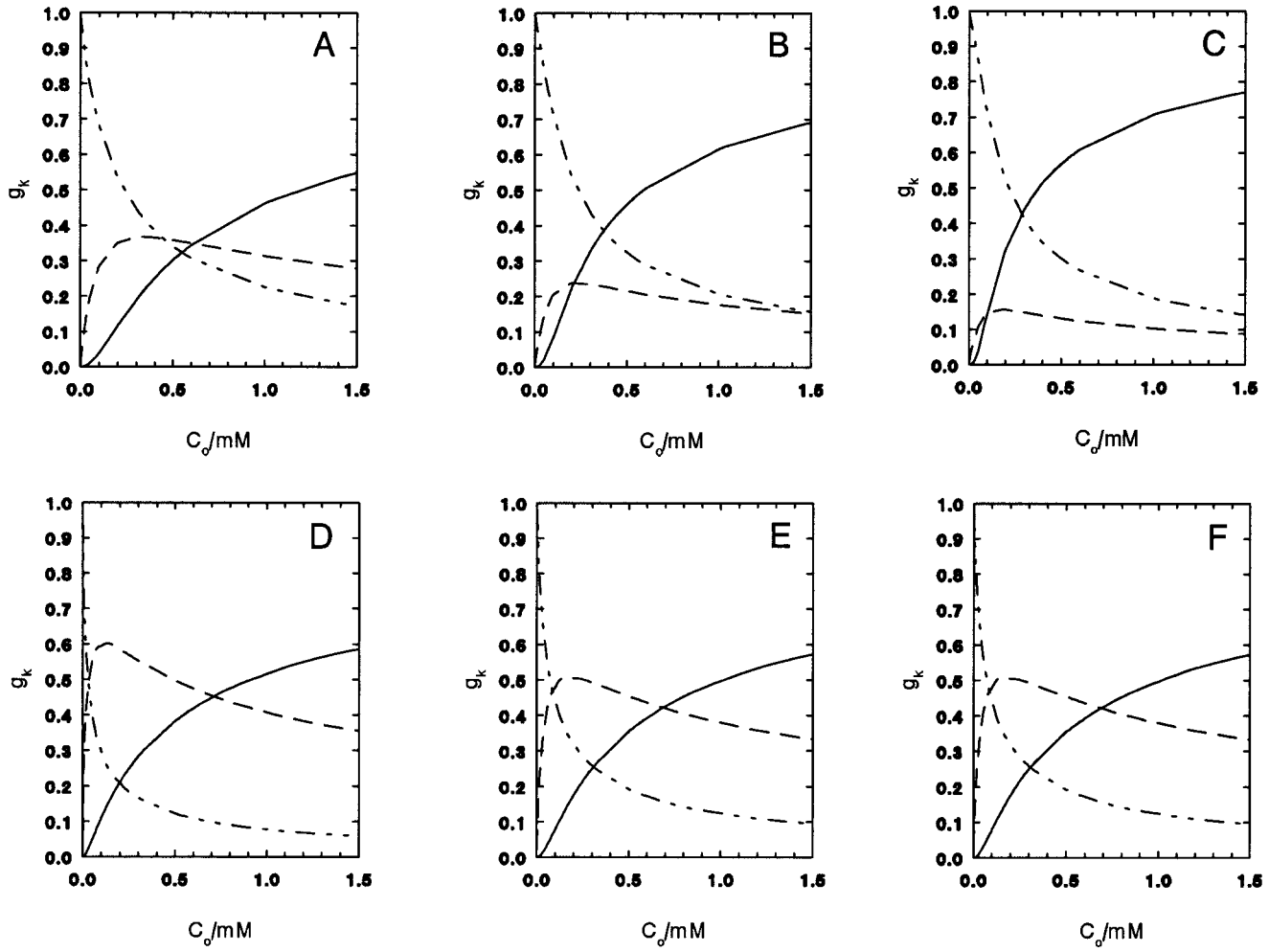

FIGURE 8 Weight fractions of oligomeric species versus total peptide formality (mM as chains) from dissociation equilibrium constants. For all: – · –, monomers; – – –, dimers; ——, tetramers. (*A–C*) For r-GCN4-lzK at 2.2, 20, and 37°C, respectively. (*D–F*) For mr-GCN4-lzK at 2.2, 20, and 37°C, respectively.

predicts that the corresponding retro-D-peptide would also form a right-handed α-helix. The argument is appealingly simple and, if verified, would represent a far-reaching and powerful theorem, because parity conservation then immediately requires that the corresponding pro-D-peptide and the retro-L-peptide each form a left-handed helix. Thus the prediction maintains that our retro-L-peptide should form a left-handed helical dimeric coiled coil with a right-handed supertwist. Although it is not quite clear what the CD of a left-handed α-helix made of L-amino acids would look like, one can be sure that this is not the explanation of our data. The lack of stability of the entire structure and the observation of tetramers at low to moderate T argues strongly against such an explanation.

The second idea therefore also fails. In this case, the prediction may fail partly because it omits consideration of the heptad composition in coiled coils, a composition that is altered by retro expression, as noted above and earlier (Liu et al., 1998). However, the failure must be far wider in scope than the family of coiled coils, in part because the argument also ignores the alterations retro expression introduces in side-chain–backbone interactions. As noted above, in a sequence segment such as —LIVE—made from L-amino acids, the valine side chain points in the general direction of the isoleucine. In the corresponding retropeptide made of D-amino acids, this valine also points toward the isoleucine. However, that direction is now C-wards rather than N-wards in the chain, so interaction with the helix dipole is reversed. Thus the correspondence of pro-L-peptides with retro-D-peptides is inexact.

Finally, an even more general argument, based on homopolypeptide studies, immediately shows that the theorem must fail. It has been known for decades that the poly(L-glutamic acid) homopolymeric chain forms a stable right-handed α-helix in acidic aqueous solutions. The theorem therefore predicts that retropoly(L-glutamic acid) should

form a left-handed α-helix. Yet retro- and propoly(L-glutamic acid) are identical and must have the same conformation. Thus, in this simplest of instances, the theorem reduces to an absurdity.

What, then, is the cause of the CD extremum at 222 nm in the case of r-GCN4-lzK, a hint of which also appears in its mutant? To answer this, we require information on the individual contributions to the CD of the three oligomeric species. Although we, perforce, measure only the total CD, such a decomposition can be effected by using the ultracentrifuge results in conjunction with the CD. The total mean residue ellipticity at 222 nm is given by

$$[\Theta_{222}] = g_1[\Theta_{222}]_1 + g_2[\Theta_{222}]_2 + g_4[\Theta_{222}]_4, \qquad (5)$$

wherein g_k is the weight fraction of k-mer and $[\Theta_{222}]_k$ is its mean residue ellipticity at 222 nm. The ultracentrifuge results give us the equilibrium constants, which relate the concentrations of monomer, dimer, and tetramer as functions of T. Knowing also the total concentration, we can calculate the weight fractions, g_k, for all three species at any given temperature. The resulting values are shown in Fig. 8 for the three temperatures employed in the ultracentrifuge experiments.

At any given T, the value of the 222-nm mean residue ellipticity of each oligomeric species is a constant, but the relative fraction of each varies with concentration, so the measured value of $[\Theta_{222}]$ also varies with concentration, as required by Eq. 5. This observed variation is shown for r-GCN4-lzK in Fig. 9 and for mr-GCN4-lzK in Fig. 10. These data can be fit to Eq. 5, by linear least squares, using the appropriate g_k values from the ultracentrifuge data (Fig. 8). These are shown as the curves in Figs. 9 and 10 for the three temperatures 2, 20, and 37°C. These fits provide values of the individual $[\Theta_{222}]_k$ for each of the three species. These individual ellipticities are shown in Figs. 11 and 12 for the retropeptide and its mutant, respectively.

This dissection of the CD, made possible by the simultaneous availability of ultracentrifuge data, allows us to draw conclusions about the individual conformations of the monomer, dimer, and tetramer populations that would be impossible to obtain from CD alone. For the r-GCN4-lzK peptide (Fig. 11), it is apparent that the monomer mean residue ellipticity at 222 nm is about -50 deg-cm^2/mmol, a value that indicates very little, but perhaps not zero, helix content and is essentially independent of T. This result is also directly apparent from the measured CD itself (Fig. 5), because at the lowest concentration (3 μM) the system is essentially all monomer.

As Fig. 11 also shows, the dimer population actually increases in helicity between 2 and 20°C, before declining sharply when the temperature is further raised to 37°C. The value at 20°C indicates that the dimer ensemble there comprises molecules that are virtually completely helical. The tetramer population also has a high helix content but shows more conventional behavior, declining modestly with T from low to room temperature and more slowly from there to 37°C. The apparent "cold denaturation," i.e., the unfolding of the dimer as the temperature is lowered from room temperature to low values, has previously been observed with certain proteins but not, to our knowledge, in a coiled coil, the most likely conformation of our retropeptide.

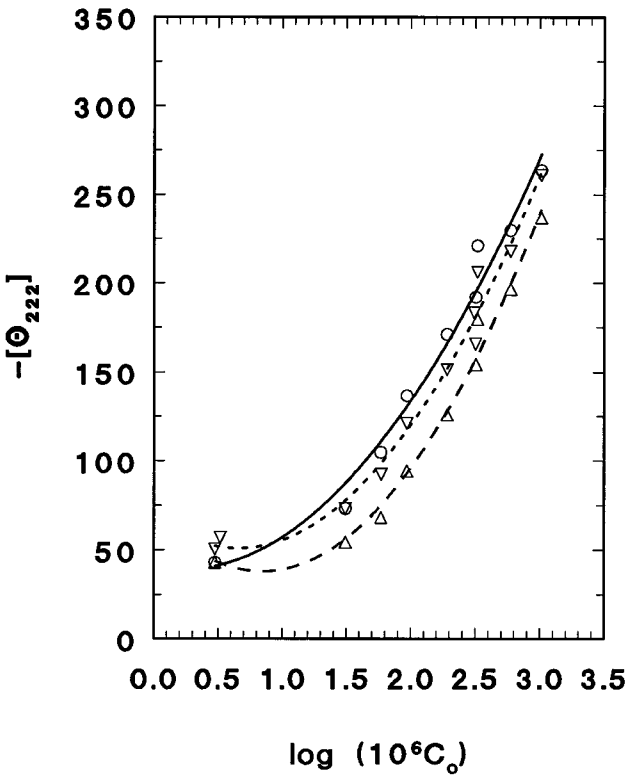

FIGURE 9 Negative of the mean residue ellipticity at 222 nm of r-GCN4-lzK versus base 10 logarithm of the total peptide formality (as chains). C_0 is in molarity units. Data points are experimental values; curves are best fits to Eq. 5. ▽ and - - - - -, 2.2°C; ○ and ——, 20°C; △ and – – –, 37°C.

The helicity of the monomeric mutant retropeptide (Fig. 12) appears to be a bit higher than that of the unmutated retropeptide (Fig. 11) and displays a slight helicity increase in the range 0 -20°C. This higher value for monomeric mr-GCN4-lzK at lower temperatures, compared with the limits approached at very high temperatures (Fig. 6), suggests that, unlike the r-GCN4-lzK monomers, those of mr-GCN4-lzK unfold significantly above room temperature. A comparison of Figs. 11 and 12 also shows that the tetramers of mr-GCN4-lzK have lower and more temperature-sensitive helical content than their r-GCN4-lzK counterparts. The mr-GCN4-lzK dimers are virtually completely helical and show a hint of the maximum at 20°C that is more strikingly apparent in r-GCN4-lzK. The helicity of mutant dimers drops less sharply with temperature above 20°C than that of the unmutated retropeptide.

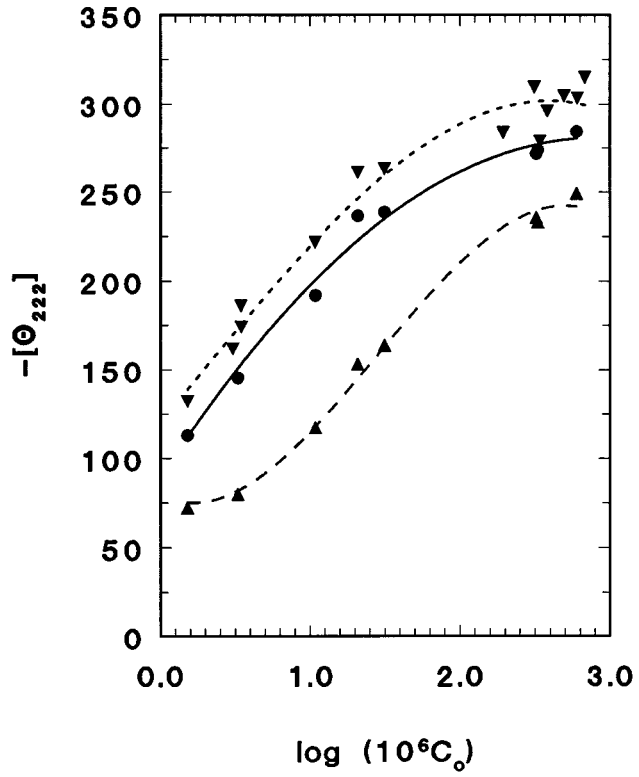

FIGURE 10 Negative of the mean residue ellipticity at 222 nm of mr-GCN4-lzK versus base 10 logarithm of the total peptide formality (as chains). C_0 is in molarity units. Data points are experimental values; curves are best fits to Eq. 5. ▼ and - - - - -, 2.2°C; ● and ——, 20°C; ▲ and – – –, 37°C.

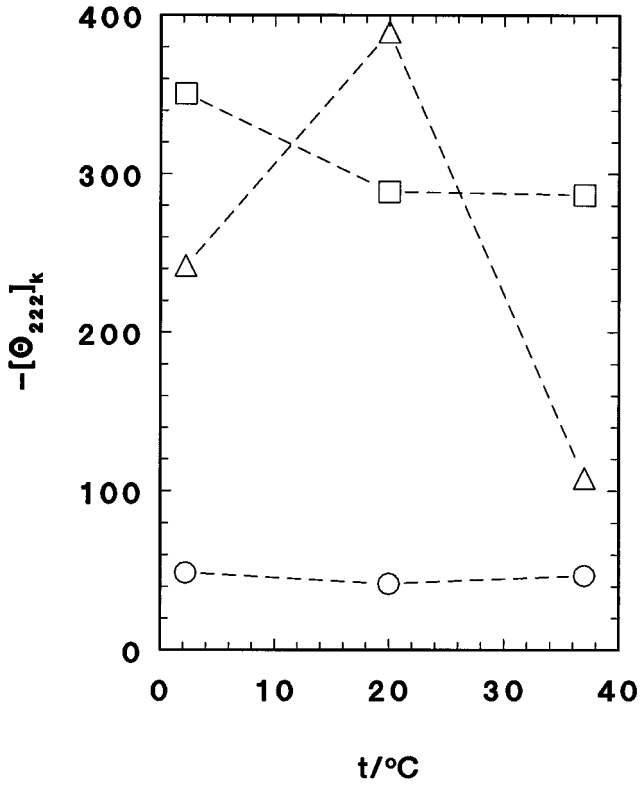

FIGURE 11 Intrinsic mean residue ellipticity at 222 nm of oligomeric species of r-GCN4-lzK versus Celsius temperature. All points are as obtained from best fit to Eq. 5. ○, Monomer; △, dimer; □, tetramer. Dashed lines are used simply to guide the eye between points for a given oligomer.

The decomposition of the CD shown in Fig. 11 helps reveal the cause of the maximum in $-[\Theta_{222}]$ that is observed in the retropeptide. Armed with the individual values of the species ellipticities, we can calculate the individual contributions they make to the overall observed ellipticity, i.e., $g_k[\Theta_{222}]_k$. These are shown for r-GCN4-lzK at 192 μM in Fig. 13 *A*. With a change from 2 to 20°C, the value of the measured quantity $-[\Theta_{222}]$ becomes more positive by ~29 deg-cm^2/mmol. Of that total change, monomers provide almost nothing, and that in the opposite direction (−3), because neither their amount nor their intrinsic CD changes much. Dimers, on the other hand, actually decline in amount (from 35 to 24%), but the increase in $-[\Theta_{222}]_2$ leads to an increase in their contribution by +8. For tetramers, the intrinsic value of $-[\Theta_{222}]_4$ actually declines, but tetramers increase in weight fraction, leading to a net change of +24 deg-cm^2/mmol. Thus dimers are responsible for about one-fourth of the total increase in $-[\Theta_{222}]$ in the low to room temperature region and tetramers for about three-fourths, but they do so for opposite reasons.

A maximum in $-[\Theta_{222}]$ is also seen in the mutant mr-GCN4-lzK, but it is shallower, shifts to near 6°C, and disappears at higher concentrations. Our decomposition of the CD also provides an explanation of those findings. As Fig. 13 *B* shows (for 330 μM), the monomer and dimer contributions increase somewhat in the 0–6°C range. The tetramer contribution falls monotonically. The relative constancy observed in mr-GCN4-lzK in this range of *T* must therefore be due to the small increases in the monomer and dimer contributions. Because the weight fraction of dimer actually declines from 33% to 16% in this temperature range, its net effect must be caused by the increase in helicity of the dimer ensemble, as seen in Fig. 12. The maximum in the observed $-[\Theta_{222}]$ disappears at higher concentrations, because there the principal oligomeric species becomes the tetramer, with its monotonically falling helicity. That these remarkable differences between r-GCN4-lzK and its mutant could be caused by permutation of only two residues constitutes a pointed challenge for conformational theory.

An alternative explanation of these observed extrema is possible. If some left-handed helices do indeed form in these solutions at the lowest temperatures, and if they have smaller values of $-[\Theta_{222}]$ and are less thermally stable than right-handed ones, then they could also cause such an extremum. We do not think this alternative scenario is very likely, however.

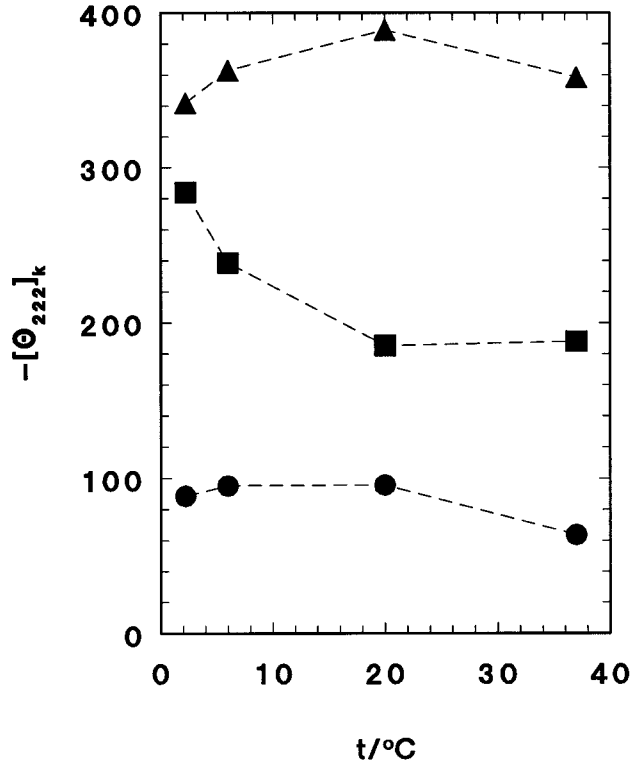

FIGURE 12 Intrinsic mean residue ellipticity at 222 nm of oligomeric species of mr-GCN4-lzK versus Celsius temperature. All points are as obtained from best fit to Eq. 5. ●, Monomer; ▲, dimer; ■, tetramer. Dashed lines are used simply to guide the eye between points for a given oligomer.

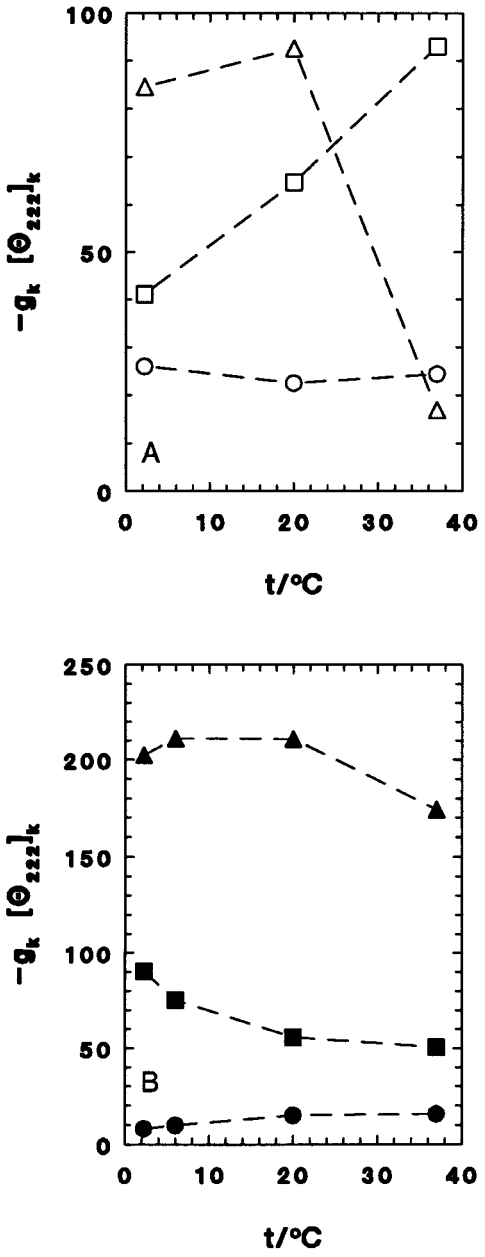

FIGURE 13 Contribution of various oligomeric species to the observed negative of the mean residue ellipticity at 222 nm versus Celsius temperature. (*A*) r-GCN4-lzK at 192 μM. ○, Monomer; △, dimer; □, tetramer. (*B*) mr-GCN4-lzK at 330 μM. ●, Monomer; ▲, dimer; ■, tetramer.

It remains to compare our findings with those of the only other study of retro-coiled coils (Liu et al., 1998). Two peptides were studied: 1) r-LZ35, a retro-GCN4-lz, with a dimeric QL sequence added to the C-terminus, and 2) r-LZ38, an r-LZ35 chain with a CGG sequence added to the N-terminus. The latter allowed the study of a disulfide-cross-linked version. Some of their results are similar to ours. Their non-cross-linked peptide, rLZ35, displays a monomer-tetramer equilibrium but differs in that no stable dimeric species was observed in their ultracentrifuge experiments. Their studies of CD versus protein concentration or guanidinium concentration also point to limited stability of the folded, highly helical oligomers. However, it is probably unwise to attempt to compare these two studies in more detail, because of the following fundamental differences. First, our experiments did not include any disulfide-cross-linked species. Second, theirs were confined to a single temperature (23°C), so they could not have seen any extremum in the CD at 222 nm, as observed in our study. Third, although Liu et al. display both CD and ultracentrifuge data, albeit at one temperature, they do not perform any dissection of the CD into contributions from individual oligomeric species. Fourth, and most important, the solvent media employed in the two studies differ drastically. Our experiments were in the common neutral saline phosphate buffer, $(NaCl)_{100}(NaPi)_{50}(7.4)$. Their experiments were in $(KCl)_{80}(Tris\text{-}HCl)_{20}(5.0)$. The latter is a rather odd medium in that only the ionic strength (100 mM) is in the usual range. The pH is far from physiological and leaves the precise charge state of the carboxyls in doubt. Because Tris(hydroxymethyl)aminomethane has no buffer capacity at such a low pH, its role is simply one of a rather unorthodox supporting electrolyte, the solutions being unbuf-

fered. These differences in solvent milieu deter further comparison, because solvent is such a strong determinant of macromolecular conformation.

CONCLUSION

The equilibrium conformation adopted by retro-expressed GCN4-like coiled coils conforms neither to the prediction that they would have a conformation similar to that of the corresponding propeptide, nor to the prediction that their conformation would be the same, but of opposite chirality. Instead, the oligomerization state of the retro version differs from that seen in the propeptide, the former including stable tetramers as well as the dimers seen in the propeptide. These differences probably result in part from perturbations introduced into the heptad structure of the chain by retroexpression, particularly the $a \leftrightarrow d$ transformation. Although the retropeptides form structures that show cooperative thermal unfolding, their thermal stability is greatly reduced from that of the propeptide parent, even in a mutant retropeptide in which an asparagine that forms an important interchain hydrogen bond in the propeptide is restored to its proper interior heptad position. Ultracentrifuge and CD data can be combined to yield information on the helix content of the individual monomer, dimer, and tetramer species. Such dissection shows that the dimeric ensemble shows a maximum in helix content between 0°C and room temperature, a phenomenon not previously seen in coiled coils. This maximum contributes to the cause of the odd empirical finding that the CD at 222 nm also has an extremum there.

The peptide synthesis portion of this work was performed at the Albert Einstein College of Medicine and was supported in part by a grant from the Mathers Foundation. The ultracentrifugation experiments were performed at the University of Connecticut and were supported by grant BIR 9318373 from the National Science Foundation. Mass spectrometry of the purified peptides was provided by the Washington University Mass Spectrometry Resource, a National Institutes of Health Research Resource (grant P41RR0954). AH acknowledges the support of the Luftmensch Society.

REFERENCES

Chorev, M., and M. Goodman. 1995. Recent developments in *retro* peptides and proteins—an ongoing topological exploration. *Trends Biotechnol.* 13:438–445.

Cohn, E. J., and J. T. Edsall. 1943. Proteins, Amino Acids, and Peptides. Reinhold, New York. 370–381.

Crick, F. 1953. The Fourier transform of a coiled coil. *Acta Crystallogr.* 6:689–697.

d'Avignon, D. A., G. L. Bretthorst, M. E. Holtzer, and A. Holtzer. 1998. Site-specific thermodynamics and kinetics of a coiled-coil transition by spin inversion transfer NMR. *Biophys. J.* 74:3190–3197.

d'Avignon, D. A., G. L. Bretthorst, M. E. Holtzer, and A. Holtzer. 1999. Thermodynamics and kinetics of a folded-folded' transition at valine-9 of a GCN4-like leucine zipper. *Biophys. J.* 76:2752–2759.

Guptasarma, P. 1992. Reversal of peptide backbone direction may result in the mirroring of peptide structure. *FEBS Lett.* 310:205–210.

Harbury, P. B., T. Zhang, P. S. Kim, and T. Alber. 1993. A switch between two-, three- and four-stranded coiled coils in GCN4 leucine zipper mutants. *Science.* 262:1401–1407.

Holtzer, M. E., D. L. Crimmins, and A. Holtzer. 1995. Structural stability of short subsequences of the tropomyosin chain. *Biopolymers.* 35: 125–136.

Holtzer, M. E., E. G. Lovett, D. A. d'Avignon, and A. Holtzer. 1997. Thermal unfolding in a GCN4-like leucine zipper: $^{13}C^{\alpha}$-NMR chemical shifts and local unfolding equilibria. *Biophys. J.* 73:1031–1041.

Ido, Y., A. Vidigni, K. Chang, R Chance, W. F. Heath, R. D. DiMarchi, E DiCera, and J. R. Williamson. 1997. Prevention of vascular and neural dysfunction in diabetic rats by C-peptide. *Science.* 277:563–566.

Johnson, M. L., J. J. Correia, H. R. Halvorson, and D. A. Yphantis. 1981. Analysis of data from the analytical ultracentrifuge by nonlinear least squares techniques. *Biophys. J.* 36:575–588.

Liu, N., C. Deillon, S. Klauser, B. Gutte, and R. M. Thomas. 1998. Synthesis, physicochemical characterization, and crystallization of a putative *retro*-coiled coil. *Protein Science*. 7:1214–1220.

Lovett, E. G., D. A. d'Avignon, M. E. Holtzer, E. H. Braswell, D. Zhu, and A. Holtzer. 1996. Observation via one-dimensional $^{13}C^{\alpha}$-NMR of local conformational substates in thermal unfolding equilibria of a synthetic analog of the GCN4 leucine zipper. *Proc. Natl. Acad. Sci. USA.* 93: 1781–1785.

Lumb, K. J., and P. S. Kim. 1995. A buried polar interaction imparts structural uniqueness in a designed heterodimeric coiled coil. *Biochemistry*. 34:8642–8648.

Lupas, A. 1996. Coiled coils: new structures and new functions. *Trends Biochem. Sci.* 21:375–382.

McDonnell, J. M., D. Fushman, S. M. Cahill, B. J. Sutton, and D. Cowburn. 1997. Solution structures of FcϵRI α-chain mimics: a β-hairpin peptide and its retroenantiomer. *J. Am. Chem. Soc.* 119:5321–5328.

McLachlan, A. D., and M. Stewart. 1975. Tropomyosin coiled-coil interactions: evidence for an unstaggered structure. *J. Mol. Biol.* 98: 293–304.

Olszewski, A., A. Kolinski, and J. Skolnick. 1996. Does a backwardly read protein sequence have a unique native state? *Protein Eng.* 9:5–15.

O'Shea, E. K., J. D. Klemm, P. S. Kim, and T. Alber. 1991. X-ray structure of the GCN4 leucine zipper, a two-stranded coiled coil. *Science.* 254: 539–544.

O'Shea, E. K., R. Rutkowski, and P. S. Kim. 1989. Evidence that the leucine zipper is a coiled coil. *Science.* 243:538–542.